Improved Capacity Scaling in Wireless Networks With Infrastructure

Won-Yong Shin, *Member, IEEE,* Sang-Woon Jeon, *Student Member, IEEE,*
Natasha Devroye, Mai H. Vu, *Member, IEEE,*
Sae-Young Chung, *Senior Member, IEEE,* Yong H. Lee, *Senior Member, IEEE,*
and Vahid Tarokh, *Senior Member, IEEE*

The work of W.-Y. Shin and Y. H. Lee was supported by the Brain Korea 21 Project, The School of Information Technology, KAIST in 2008. The work of S.-W. Jeon and S.-Y. Chung was supported by the MKE under the ITRC support program supervised by the IITA (IITA-2008-C1090-0803-0002). The work of M. H. Vu was supported in part by ARO MURI grant number W911NF-07-1-0376. The material in this paper was presented in part at the IEEE Communication Theory Workshop, St. Croix, US Virgin Islands, May 2008 and the IEEE International Symposium on Information Theory, Toronto, Canada, July 2008.

W.-Y. Shin, S.-W. Jeon, S.-Y. Chung, and Y. H. Lee are with the School of EECS, KAIST, Daejeon 305-701, Korea (E-mail: wyshin@stein.kaist.ac.kr; swjeon@kaist.ac.kr; sychung@ee.kaist.ac.kr; yohlee@ee.kaist.ac.kr).

N. Devroye was with the School of Engineering and Applied Sciences, Harvard University, Cambridge, MA 02138 USA. She is now with the Department of Electrical and Computer Engineering, University of Illinois at Chicago, Chicago, Illinois 60607 USA (E-mail: devroye@ece.uic.edu).

M. H. Vu and and V. Tarokh are with the School of Engineering and Applied Sciences, Harvard University, Cambridge, MA 02138 USA (E-mail: maivu@seas.harvard.edu; vahid@seas.harvard.edu).

Abstract

This paper analyzes the impact and benefits of infrastructure support in improving the throughput scaling in networks of n randomly located wireless nodes. The infrastructure uses multi-antenna base stations (BSs), in which the number of BSs and the number of antennas at each BS can scale at arbitrary rates relative to n. Two schemes are introduced in this study: a BS-based single-hop routing protocol with multiple-access uplink and broadcast downlink and a BS-based multi-hop routing protocol. Then, the throughput scaling laws of each are analyzed here. These schemes are compared against two conventional schemes without BSs: the multi-hop (MH) transmission and hierarchical cooperation (HC) schemes. It is shown that the BS-based routing schemes do not improve the throughput scaling in dense networks. In contrast, the proposed BS-based routing schemes can, under realistic network conditions, improve the throughput scaling significantly in extended networks. The gain comes from the following advantages of these BS-based protocols. First, more nodes can transmit simultaneously in the proposed scheme than in the the MH scheme if the number of BSs and the number of antennas are large enough. Second, by improving the long-distance signal-to-noise ratio (SNR), the received signal power may be larger than that of the HC, allowing for a better throughput scaling under extended networks. Furthermore, by deriving the corresponding information-theoretic cut-set upper bounds, it is shown that, for all the operating regimes, the achievability results are order-optimal.

I. INTRODUCTION

In [1], Gupta and Kumar introduced and studied the throughput scaling in a large wireless ad hoc network. They showed that, for a network of n source-destination (S-D) pairs randomly distributed in a unit area, the total throughput scales as $\Theta(\sqrt{n/\log n})$.[1] This throughput scaling is achieved using a multi-hop (MH) communication scheme. Recent results have shown that an almost linear throughput in the network, i.e., $\Theta(n^{1-\epsilon})$ for an arbitrarily small $\epsilon > 0$, is achievable by using a hierarchical cooperation (HC) strategy [3], [4], [5], [6]. Besides the schemes in [3], [4], [5], [6], there has been a steady push to improve the throughput of wireless networks up to a linear scaling in a variety of network scenarios by using novel techniques such as networks with node mobility [7], interference alignment schemes [8], and infrastructure support [9].

Although it would be good to have such a linear scaling with only wireless connectivity, in practice there will be a price to pay in terms of higher delay and higher cost of channel estimation. For these reasons, it would still be good to have infrastructure aiding wireless nodes. Such hybrid networks consisting of both wireless ad hoc nodes and infrastructure nodes, or equivalently base stations (BSs), have been introduced and analyzed in [10], [11], [9], [12], [13]. BSs are assumed to be interconnected by high capacity wired links. It is strictly necessary for the number m of BSs to exceed a threshold in order to obtain a linear throughput scaling in m.

While it has been shown that BSs can be beneficial in wireless networks, the impact and benefits of infrastructure support are not yet fully understood. This paper features analysis of the throughput scaling laws for a more general hybrid network where there are l antennas at each BS, allowing the exploitation of the spatial dimension at each BS.[2] By allowing the number m of BSs and the number l of antennas to scale at arbitrary rates relative to the number n of wireless nodes, achievable scaling rates and information-theoretic upper bounds are derived as a function of these scaling parameters. Two new routing protocols utilizing BSs are proposed here. In the first protocol, multiple sources (nodes) transmit simultaneously to each BS using a direct single-hop multiple-access in the uplink and a direct single-hop broadcast from each BS in the downlink. In the second protocol, the high-speed BS links are combined with nearest-neighbor routing via MH among the wireless nodes. The obtained results are also compared to two conventional schemes without using BSs: the MH protocol [1] and HC protocol [3].

The proposed schemes are evaluated in two different networks: dense networks [1], [14], [3] of unit area, and extended networks [15], [16], [17], [18], [3] of unit node density. In dense networks, it is shown that the presence of the BSs does not improve the throughput scaling and the HC always outperforms the other protocols. On the contrary, in extended networks, depending on the network configurations and the path-loss attenuation, the proposed BS-based protocols can improve the throughput scaling significantly. Part of the improvement comes from the following two advantages over the conventional schemes: having more antennas enables more transmit pairs that can be activated simultaneously (compared to those of the MH scheme), i.e., enough degree-of-freedom (DoF) gain is obtained, provided the number m of BSs and the number l of antennas per BS are large enough. In addition, the BSs help to improve the long-distance signal-to-noise ratio (SNR)[3], first termed in [19], which leads to a larger received signal power than that of the HC scheme, i.e., the power gain is obtained, thus allowing for a better throughput scaling in extended networks.

To assess the optimality of our proposed schemes in a network with infrastructure, cut-set upper bounds on the throughput scaling are derived. For pure ad hoc networks with no BSs, upper bounds are shown in [15], [16], [20], [17], [21], [3], but those for BS-based networks are not rigorously characterized in

[1]We use the following notations: i) $f(x) = O(g(x))$ means that there exist constants C and c such that $f(x) \leq Cg(x)$ for all $x > c$. ii) $f(x) = o(g(x))$ means $\lim_{x\to\infty} \frac{f(x)}{g(x)} = 0$. iii) $f(x) = \Omega(g(x))$ if $g(x) = O(f(x))$. iv) $f(x) = \omega(g(x))$ if $g(x) = o(f(x))$. v) $f(x) = \Theta(g(x))$ if $f(x) = O(g(x))$ and $g(x) = O(f(x))$ [2].

[2]When the carrier frequency is very high, it is possible to deploy many antennas at each BS since the wavelength is small.

[3]In [19], the long-distance SNR is defined as n times the received SNR between two farthest nodes across the largest scale in wireless networks. In our BS-based network, it can be interpreted as the total SNR transferred to any given node (or BS antenna) over a certain scale reduced by infrastructure support.

both dense and extended networks. In dense networks, it is shown that the obtained upper bound is the same as that of [3] assuming no BSs. In extended networks, the proposed approach is based in part on the characteristics at power-limited regimes shown in [3], where an upper bound is proportional to the total received signal power from source nodes. It is shown under extended networks that our upper bounds match the achievable throughput scalings for all the operating regimes within a factor of n with arbitrarily small exponent.

The rest of this paper is organized as follows. Section II describes the proposed network model with infrastructure support. The two proposed BS-based protocols are characterized in Section III and their achievable throughput scalings are analyzed in Section IV. The corresponding information-theoretic cut-set upper bounds are derived in Section V. Finally, Section VI summarizes this paper with some concluding remarks.

Throughout this paper the superscript † denotes the conjugate transpose of a matrix, $\mathbf{I}_n$ is the identity matrix of size $n \times n$, $[\cdot]_{ki}$ is the (k,i)-th element of a matrix, and $\mathbb{C}$ is the field of complex numbers. $E[\cdot]$, $\mathrm{tr}(\cdot)$, and $\det(\cdot)$ are the expectation, the trace, and the determinant, respectively. Unless otherwise stated, all logarithms are assumed to be to the base 2.

II. System and Channel Models

Consider a two-dimensional wireless network that consists of n S-D pairs uniformly and independently distributed on a square except for the area covered by BSs. Then, no nodes are physically located inside the BSs. The network is assumed to have an area of one and n in dense and extended networks, respectively. Suppose that the whole area is divided into m square cells, each of which is covered by one BS with l antennas at its center (see Fig. 1). Parameters n, m, and l are related according to

$$n = m^{1/\beta} = l^{1/\gamma}, \tag{1}$$

where $\beta, \gamma \in [0,1)$ satisfying $\beta + \gamma \leq 1$. The number of antennas is allowed to grow with the number of nodes and BSs in the network. The placement of these l antennas depends on how the number of antennas scales as follows:

1) l antennas are regularly placed on the BS boundary if $l = O(\sqrt{n/m})$, and
2) $\sqrt{n/m}$ antennas are regularly placed on the BS boundary and the rest are uniformly placed inside the boundary if $l = \omega(\sqrt{n/m})$ and $l = O(n/m)$.[4]

Furthermore, it is assumed that the BS-to-BS links have infinite capacity and that these BSs are neither sources nor destinations. It is supposed that the radius of each BS scales as $\epsilon_0/\sqrt{m}$ for dense networks and as $\epsilon_0\sqrt{n/m}$ for extended networks, where $\epsilon_0 > 0$ is an arbitrarily small constant independent of n, which means it is independent of m and l as well. This radius scaling would ensure enough separation among the antennas since the per-antenna distance scales at least as the average per-node distance for any parameters n, m, and l.

The signal model in the uplink will be described first. Let $I \subset \{1, \cdots, n\}$ denote the set of simultaneously transmitting wireless nodes. Then, the $l \times 1$ received signal vector $\mathbf{y}_s$ at BS $s \in \{1, \cdots, m\}$ and the $l \times 1$ complex channel vector $\mathbf{h}_{si}^u$ between node $i \in \{1, \cdots, n\}$ and BS s are given by

$$\mathbf{y}_s = \sum_{i \in I} \mathbf{h}_{si}^u x_i + \mathbf{n}_s \tag{2}$$

and

$$\mathbf{h}_{si}^u = \left[\frac{e^{j\theta_{si,1}^u}}{r_{si,1}^{u\ \alpha/2}} \ \frac{e^{j\theta_{si,2}^u}}{r_{si,2}^{u\ \alpha/2}} \cdots \ \frac{e^{j\theta_{si,l}^u}}{r_{si,l}^{u\ \alpha/2}} \right]^T, \tag{3}$$

[4]Such an antenna deployment guarantees both the nearest neighbor transmission from/to each BS antenna and the enough space among the antennas.

respectively, where x_i is the signal transmitted by the i-th node, and $\mathbf{n}_s$ denotes the circularly symmetric complex additive white Gaussian noise (AWGN) vector whose element has zero-mean and variance N_0. T denotes the transpose of a vector, and $\theta^u_{si,t}$ represents the random phases uniformly distributed over $[0, 2\pi]$ and independent for different i, s, t, and time (transmission symbol), i.e., fast fading. Note that this random phase model is based on a far-field assumption, which is valid if the wavelength is sufficiently small. $r^u_{si,t}$ and $\alpha > 2$ denote the distance between node i and the t-th antenna of BS s, and the path-loss exponent, respectively. Similarly, the $1 \times l$ complex channel vector in the downlink, $\mathbf{h}^d_{is}$ between BS $s \in \{1, \cdots, m\}$ and node $i \in \{1, \cdots, n\}$, and the complex channel h_{ki} between nodes i and k ($i, k \in \{1, \cdots, n\}$) are given by

$$\mathbf{h}^d_{is} = \left[\frac{e^{j\theta^d_{is,1}}}{r^{d\ \alpha/2}_{is,1}} \ \frac{e^{j\theta^d_{is,2}}}{r^{d\ \alpha/2}_{is,2}} \cdots \ \frac{e^{j\theta^d_{is,l}}}{r^{d\ \alpha/2}_{is,l}} \right] \tag{4}$$

and

$$h_{ki} = \frac{e^{j\theta_{ki}}}{r^{\alpha/2}_{ki}}, \tag{5}$$

respectively, where $\theta^d_{is,t}$ and θ_{ki} have uniform distribution over $[0, 2\pi]$, and are independent for different i, s, t, k, and time. $r^d_{is,t}$ and r_{ki} denote the distance between the t-th antenna of BS s and node i, and the distance between nodes i and k, respectively.

Suppose that each node has an average transmit power constraint P (constant). It is assumed that the total transmit power at each BS is constrained to scale linearly with the number of nodes covered by one cell. Channel state information (CSI) is assumed to be available at the receivers but not at the transmitters (unless otherwise stated). It is assumed that each node transmits at a rate $T_n(\alpha, \beta, \gamma)/n$, where $T_n(\alpha, \beta, \gamma)$ denotes the total throughput of the network.

III. Routing Protocols

This section explains the two BS-based protocols in the network. Two conventional schemes [1], [3] with no infrastructure support are also described.

A. Protocols With Infrastructure Support

We generalize the conventional BS-based transmission scheme in [10], [11], [9], [12], [13]: a source node transmits its packet to the closest BS, the BS having the packet transmits it to the BS that is nearest to the destination of the source via wired BS-to-BS links, and the destination finally receives its data from the nearest BS. Since there exist both access (to BSs) and exit (from BSs) routings, different time slots are used, e.g., even and odd time slots, respectively. We start from the following lemma.

Lemma 1: Suppose $m = n^\beta$ where $\beta \in [0, 1)$. Then, the number of nodes inside each cell is between $((1 - \delta_0)n^{1-\beta}, (1 + \delta_0)n^{1-\beta})$, i.e., $\Theta(n/m)$, with high probability (whp) for some constant $0 < \delta_0 < 1$ independent of n.

The proof of this lemma is given by slightly modifying the asymptotic analysis in [3].

1) Infrastructure-supported single-hop (ISH) protocol: In contrast with previous works, the spatial dimensions enabled by having multiple antennas at each BS are exploited here, and thus multiple transmission pairs can be supported using a single BS. An infrastructure-supported single-hop (ISH) transmission protocol shown in Fig. 2 under dense networks is now proposed as follows:

- Divide the network into square cells of area $1/m$ having one BS at the center of each cell.
- For the access routing, all source nodes in each cell, given by n/m nodes whp from Lemma 1, transmit their independent packets simultaneously via single-hop multiple-access to the BS in the same cell. A transmit power of $\frac{P}{(n/m)m^{\alpha/2}}$ is used at each node for uplink transmission (how to exploit full DoF in the uplink with this transmit power will be rigorously analyzed later).

- Each BS receives and jointly decodes packets from source nodes in the same cell and treats signals received from the other cells as noise. Each BS performs a minimum mean-square error (MMSE) estimation [22], [23], [24] with successive interference cancellation (SIC), which is one of receive filters, in the uplink. More precisely, the $l \times 1$ unnormalized receive filter $\mathbf{v}_i$ has the expression [23]

$$\mathbf{v}_i = \left(\mathbf{I}_l + \sum_{k>i} \frac{P}{nm^{\alpha/2-1}} \mathbf{h}_{sk}^u \mathbf{h}_{sk}^{u\,\dagger} \right)^{-1} \mathbf{h}_{si}^u, \tag{6}$$

  which means that the receiver of BS s for the i-th node cancels signals from nodes $1, \cdots, i-1$ and treats signals from nodes $i+1, \cdots, n/m$ as noise, for every i, when the canceling order is $1, \cdots, n/m$.
- The BS that completes decoding its packets transmits them to the BS closest to the corresponding destination by wired BS-to-BS links.
- For the exit routing, each BS transmits all received packets, i.e., n/m packets, via single-hop broadcast to the destinations in the cell. The transmitters in the downlink are designed by the dual system [23], [24] of MMSE-SIC receive filters in the uplink, and thus perform an MMSE transmit precoding $\mathbf{u}_1, \cdots, \mathbf{u}_{n/m}$ with dirty paper coding [25], [26], [27] at BS s:

$$\mathbf{u}_i = \left(\mathbf{I}_l + \sum_{k>i} p_k \mathbf{h}_{ks}^{d\,\dagger} \mathbf{h}_{ks}^d \right)^{-1} \mathbf{h}_{is}^{d\,\dagger}, \tag{7}$$

  where the power $p_k \geq 0$ allocated to each node satisfies $\sum_k p_k \leq \frac{P}{m^{\alpha/2}}$ for $k = 1, \cdots, n/m$.[5] Note that a total transmit power of $\frac{P}{m^{\alpha/2}}$ is used at each BS for downlink transmission. The CSI at the transmitter is only required at each BS to perform a transmit precoding in the downlink.

For the ISH protocol, more DoF gain is provided compared to transmissions via MH if m and l are large enough. The power gain can also be obtained compared to that of the HC scheme in certain cases.

Note that when $\alpha > 2$ the transmit power $\frac{P}{(n/m)m^{\alpha/2}}$ at each node tends to zero as $n \to \infty$ (equivalently, $m \to \infty$). Hence, the given protocol satisfies the average power constraint P in the uplink. Similarly, it is easily shown that the average power constraint at each BS is satisfied in the downlink.

For extended networks, the above protocol can be directly applied by scaling the area by n. If $(n/m)(m/n)^{\alpha/2} = (m/n)^{\alpha/2-1}$ tends to zero as n tends to infinity, the network is power-limited. Hence, the proposed ISH scheme is used with the full power, i.e., the transmit powers at each node and BS are P and $\frac{nP}{m}$, respectively. In this case, the throughput will decrease by $(m/n)^{\alpha/2-1}$ compared to the dense network case. (Note that this relies on the fact that $\log(1+x)$ can be approximated by x for small $x > 0$.) Based on this observation, the achievable throughput can be analyzed in a manner similar to that for dense networks. However, instead of original (continuous) transmissions, a bursty transmission scheme [3], [19], that uses only a fraction $(m/n)^{\alpha/2-1}$ of the time for actual transmission with instantaneous power $\frac{P}{(m/n)^{\alpha/2-1}}$ and $\frac{(n/m)P}{(m/n)^{\alpha/2-1}}$ per node and BS, respectively, is used to simply apply the analysis for dense networks. Under the extended networks with the bursty ISH protocol, it may be concluded that the total throughput decreases by $(m/n)^{\alpha/2-1}$ compared to the dense network scenario.

2) Infrastructure-supported multi-hop (IMH) protocol: The fact that the extended network is power-limited motivates the introduction of an infrastructure-supported multi-hop (IMH) transmission protocol in which multiple source nodes in a cell transmit their packets to BS in the cell via MH, thereby having much higher received power than that of the direct one-hop transmission in extended networks. Similarly, each BS delivers its packets to the corresponding destinations by IMH transmissions. The proposed IMH transmission protocol in Fig. 3 under dense networks is as follows:

[5]For the exit routing, an optimal power allocation strategy is not shown in this paper since the transmission rate scaling is the same as that for the access routing by simply letting $p_1 = \cdots = p_{n/m}$, which will be discussed in the next section.

- Divide the network into square cells of area $1/m$ each and again divide each cell into smaller square cells of area $2\log n/n$ each, where these smaller cells are called routing cells (which include at least one node [1], [14]).
- For the access routing, $\min\{l, \sqrt{n/m}\}$ source nodes in each cell transmit their independent packets using MH routing (which will be described in Section III-B) to the corresponding BS. Let us now consider how to set an MH routing path from each source to the corresponding BS. Draw a line connecting a source to one of the antennas of its BS and perform MH routing horizontally or vertically by using the adjacent routing cells passing through the line until its packet reaches the corresponding receiver (antenna). Note that it is possible to draw $\min\{l, \sqrt{n/m}\}$ lines such that there are no crossings in the cell (see Fig. 4). A transmit power $P/n^{\alpha/2}$ at each node is used.
- It is assumed that each antenna placed only on the BS boundary receives its packet from one of the nodes in the nearest outer neighbor routing cell. If $l = \omega(\sqrt{n/m})$, each boundary routing cell in the BS has at least one BS antenna, and thus an arbitrary antenna inside the routing cell can receive a packet. Each receiver treats signals from the other nodes as noise, and decodes its packet independently.
- The BS-to-BS transmissions are the same as the ISH case.
- For the exit routing, the MH routing from a BS to multiple destinations similar to the above access routing is performed. Each antenna in the routing cell of the BS boundary transmits its packet to a destination via MH transmissions along a line connecting the antenna of its BS to the corresponding destination. A transmit power $P/n^{\alpha/2}$ is used at each BS antenna (which satisfies the power constraint).
- Each routing cell operates based on 9-time division multiple access (TDMA) to avoid causing huge interference to its neighbor cells.

For the IMH protocol, more DoF gain is possible compared to the MH scheme for large m and l. In addition, more power gain can also be obtained compared to the HC and ISH schemes in certain cases.

Note that the node transmit power of the given protocol satisfies the average power constraint P as n goes to infinity. The per-antenna power constraint at each BS is also satisfied.

In a manner similar to that of the ISH protocol, by converting the area of a cell to square cells of area n/m each and setting the area of a routing cell to $2\log n$ and the required transmit power at each node/BS antenna to P, it is possible to apply the IMH protocol to extended networks. Then, since the proposed IMH protocol satisfies the power constraint and thus the network is not power-limited, a total throughput does not decrease compared to the dense network case, which will be analyzed in the next section.

B. Protocols Without Infrastructure Support

To improve throughput scalings of infrastructure-supported networks, the number of BSs should be higher than a certain level. That is, pure ad hoc transmissions without help of BSs may achieve better throughput scaling when the number m of BSs is not large enough. The MH and HC protocols which were proposed in [1] and [3], respectively, will be briefly introduced.

1) MH protocol: The basic procedure of the MH protocol in dense networks is as follows:

- Divide the network into square routing cells of area $2\log n/n$.
- Draw a line connecting a S-D pair. A source transmits a packet to its destination using the nodes in the adjacent cells passing through the line.
- A transmit power of $P/n^{\alpha/2}$ is enough to guarantee the required throughput scaling of the MH protocol at each transmission.
- Each routing cell operates the 9-TDMA to avoid a large interference.

For extended networks, it is possible to apply the above protocol by converting the area of a cell to $2\log n$ and the transmit power to P.

2) HC protocol: The HC consists of three phases as follows:

- Divide the network into clusters each having $\Theta(M)$ nodes where $M = n^{\eta}$ for $0 < \eta \leq 1$.
- During the first phase, each source distributes its data to the other nodes in the same cluster.
- During the second phase, a long-range multiple-input multiple-output (MIMO) transmission between two clusters having a source and its destination is performed, one at a time.
- During the last phase, each node quantizes the received observations and delivers the quantized data to the rest of nodes in the same cluster. By collecting all quantized observations, each destination can decode its packet.

When each node transmits data within its cluster, which is performed during the first and third phases, it is possible to apply another smaller-scaled cooperation within each cluster by dividing each cluster into smaller clusters. By recursively applying this procedure, it is possible to establish the hierarchical strategy in the network. A transmit power of P/n is used in dense networks while the bursty HC scheme is performed in extended networks with instantaneous power $Pn^{\alpha/2-1}$ for a fraction $1/n^{\alpha/2-1}$ of the time.

IV. Achievable Throughput Scaling

In this section, the throughput scaling for both dense and extended networks under our routing protocols is analyzed. Although the HC in [3] provides a near-optimal throughput scaling in dense networks, it may degrade throughput scalings in extended (or power-limited) networks. As a result, the best strategy among the four schemes ISH, IMH, MH, and HC depends on the path-loss exponent α, and the scaling parameters β and γ under extended networks. The scaling exponent for these parameters is defined by [3], [19]

$$e(\alpha, \beta, \gamma) = \lim_{n \to \infty} \frac{\log T_n(\alpha, \beta, \gamma)}{\log n}, \tag{8}$$

where $T_n(\alpha, \beta, \gamma)$ is the total throughput, which captures the dominant term in the exponent of the throughput scaling.[6]

A. Dense Networks

The achievable rate of the ISH protocol in dense networks will be shown first. Since all the nodes' data passes through their respective BSs, the analysis is related to that for many-to-one channels [28], [29] (in the exit routing, it is converted to that for one-to-many channels). In particular, the transmission scheme and its achievable rate were shown in [28] for a network in which all nodes are distributed uniformly over the boundary of a circle with a unit radius and the BS with a single antenna is at the center of the circle. Let it be extended to random and general hybrid networks with m BSs, each of which has l antennas, where nodes are uniformly distributed within the unit area with m BSs. The amount of interference in the ISH scheme may now be quantified.

Lemma 2: Suppose a dense network uses the ISH protocol. Then, the total interference power in the uplink from nodes in other cells to each BS antenna is upper-bounded by $\Theta(1)$ whp. Each node also has $\Theta(1)$ interference power whp in the downlink from BSs in other cells.

Proof: First consider the uplink case. There are $8k$ interfering cells, each of which includes $\Theta(n/m)$ nodes whp, in the k-th layer l_k of the network as illustrated in Fig. 5. Let d_k denote the Euclidean distance between a given BS antenna and any node in l_k, which is a random variable. Since d_k scales as $\Theta(k/\sqrt{m})$, there exists $c_2 > c_1 > 0$ with constants c_1 and c_2 independent of n, such that $d_k = c_0 k/\sqrt{m}$, where all c_0 lies in the interval $[c_1, c_2]$. Hence, the total interference power at each BS antenna from simultaneously transmitting nodes is upper-bounded by

$$\begin{aligned} \sum_{k=1}^{\infty} \frac{P}{(n/m)m^{\alpha/2}} (8k) \frac{n}{m} \frac{m^{\alpha/2}}{(c_1 k)^{\alpha}} &= \frac{8P}{c_1^{\alpha}} \sum_{k=1}^{\infty} \frac{1}{k^{\alpha-1}} \\ &\leq \bar{c}_1, \end{aligned} \tag{9}$$

[6]To simplify notations, $T_n(\alpha, \beta, \gamma)$ will be written as T_n if dropping α, β, and γ does not cause any confusion.

where $\bar{c}_1 > 0$ is a constant independent of n. In a similar manner to the uplink case, an upper bound of the total interference power at each node in the downlink is obtained as the following:

$$\sum_{k=1}^{\infty} \frac{P}{m^{\alpha/2}} (8k) \frac{m^{\alpha/2}}{(c_1 k)^{\alpha}} \leq \bar{c}_1, \tag{10}$$

where $\bar{c}_1$ is a positive constant independent of n. ■

Using Lemma 2, the following two results, that respectively show the transmission rates for the access and exit routings, are obtained.

Lemma 3: Suppose a dense network uses the ISH protocol. Then, the rate of $\Omega(l)$ at each BS is achievable for access routing.

Proof: The signal model from nodes in each cell to the BS with multiple antennas corresponds to the single-input multiple-output (SIMO) multiple-access channel (MAC). Since the maximum Euclidean distance among links of the above SIMO MAC scales as $\Theta(1/\sqrt{m})$, it is upper-bounded by as $\delta_1/\sqrt{m}$, where $\delta_1 > 0$ is a certain constant. Let N_I denote the sum of total interference power received from the other cells and noise variance N_0. Then, the worst case noise of this channel has an uncorrelated Gaussian distribution with zero-mean and variance N_I [30], [31], which lower-bounds the transmission rate. By assuming full CSI at the receiver (BS s), the mutual information of the SIMO MAC is given by [23], [24]

$$\begin{aligned} I(\mathbf{x}_s; \mathbf{y}_s, \mathbf{H}_s) &\geq E\left[\log\det\left(\mathbf{I}_l + \frac{P}{(n/m)m^{\alpha/2}N_I}\mathbf{H}_s\mathbf{H}_s^{\dagger}\right)\right] \\ &\geq E\left[\log\det\left(\mathbf{I}_l + \frac{P}{\delta_1^{\alpha}(n/m)N_I}\mathbf{G}\mathbf{G}^{\dagger}\right)\right], \end{aligned} \tag{11}$$

where $\mathbf{x}_s$ denotes the $\frac{n}{m} \times 1$ transmit signal vector, whose elements are nodes in the cell covered by BS s, $\mathbf{y}_s$ is the $l \times 1$ received signal vector at BS s, and $\mathbf{H}_s = [\mathbf{h}_{s1}^u \ \mathbf{h}_{s2}^u \ \cdots \ \mathbf{h}_{s(n/m)}^u]$ ($\mathbf{h}_{si}^u$ for $i = 1, \cdots, n/m$ is given in (3)). $\mathbf{G}$ is the normalized matrix, whose element g_{ti} is given by $e^{j\theta_{si,t}^u}$ and represents the phase between node i and the t-th antenna of BS s. Then, the above mutual information is rewritten as

$$\begin{aligned} I(\mathbf{x}_s; \mathbf{y}_s, \mathbf{H}_s) &\geq lE\left[\log\left(1 + \frac{P}{\delta_1^{\alpha}N_I}\lambda_1\right)\right] \\ &\geq l\log\left(1 + \frac{P}{\delta_1^{\alpha}N_I}\bar{\lambda}\right)\Pr\left(\lambda_1 > \bar{\lambda}\right), \end{aligned} \tag{12}$$

where λ_1 is one chosen uniformly among the l eigenvalues of $\frac{m}{n}\mathbf{G}\mathbf{G}^{\dagger}$ and $\bar{\lambda}$ is any nonnegative constant. By the Paley-Zygmund inequality [32], it is possible to lower-bound the mutual information in the left-hand side (LHS) of (12) by following the same line as that in [3], thus yielding

$$\Pr\left(\lambda_1 > \bar{\lambda}\right) \geq \frac{\left(E\left[\bar{\lambda}\right] - \lambda_1\right)^2}{E[\lambda_1^2]} \tag{13}$$

for $0 \leq \bar{\lambda} < E[\lambda_1]$. Both $E[\lambda_1]$ and $E[\lambda_1^2]$ are computed to lower-bound (12). We get the following:

$$\begin{aligned} E[\lambda_1] &= \frac{1}{l}E\left[\mathrm{tr}\left(\frac{m}{n}\mathbf{G}\mathbf{G}^{\dagger}\right)\right] \\ &= \frac{1}{l}\frac{m}{n}\sum_{t=1}^{l}\sum_{i=1}^{n/m}E\left[|g_{ti}|^2\right] \\ &= 1 \end{aligned} \tag{14}$$

and

$$\begin{aligned}
E[\lambda_1^2] &= \frac{1}{l}E\left[\mathrm{tr}\left(\left(\frac{m}{n}\right)^2 \mathbf{G}\mathbf{G}^\dagger\mathbf{G}\mathbf{G}^\dagger\right)\right] \\
&= \frac{1}{l}\left(\frac{m}{n}\right)^2 \sum_{t,p=1}^{l}\sum_{i,q=1}^{n/m} E\left[g_{ti}g_{pi}^* g_{pq}g_{tq}^*\right] \\
&\le \frac{1}{l}\left(\frac{m}{n}\right)^2 \left[\sum_{t=1}^{l}\sum_{i,q=1}^{n/m} E\left[|g_{ti}|^2\right]E\left[|g_{tq}|^2\right] + \sum_{t,p=1}^{l}\sum_{i=1}^{n/m} E\left[|g_{ti}|^2\right]E\left[|g_{pi}|^2\right]\right] \\
&= \frac{1}{l}\left(\frac{m}{n}\right)^2 \left(l\left(\frac{n}{m}\right)^2 + l^2\frac{n}{m}\right) \\
&\le 2, \qquad (15)
\end{aligned}$$

where $*$ denotes the complex conjugate. Since N_I has a constant scaling from Lemma 2, then

$$I(\mathbf{x}_s; \mathbf{y}_s, \mathbf{H}_s) \ge \bar{c}_2 l, \qquad (16)$$

where $\bar{c}_2 > 0$ is some constant independent of n. This means that the rate of the access routing at each BS scales at least as l. This completes the proof. ■

Note that l corresponds to the DoF at each cell provided by the uplink of ISH protocol.

Lemma 4: Suppose a dense network uses the ISH protocol. Then, the exist routing has the same transmission rate as the access routing, i.e., $\Omega(l)$.

Proof: For the exit routing, the signal model from the BS with multiple antennas in one cell to nodes in the cell corresponds to the multiple-input single-output (MISO) broadcast channel (BC). From Lemma 2, it is seen that the total interference power received from the other BSs is bounded. Hence, it is possible to derive the transmission rate for the exit routing by exploiting an uplink-downlink duality [23], [24], [33], [34]. The rate of the MISO BC is then equal to that of the dual SIMO MAC with a sum power constraint. More precisely, with full CSI at the transmitter (BS) and the total transmit power $\frac{P}{m^{\alpha/2}}$ in the downlink, the mutual information of the MISO BC is lower-bounded by [23]

$$\max_{\mathbf{Q}_x \ge 0} E\left[\log\det\left(\mathbf{I}_l + \frac{1}{N_I'}\mathbf{H}_s'^{\dagger}\mathbf{Q}_x\mathbf{H}_s'\right)\right] \ge E\left[\log\det\left(\mathbf{I}_l + \frac{P}{(n/m)m^{\alpha/2}N_I'}\mathbf{H}_s'^{\dagger}\mathbf{H}_s'\right)\right], \qquad (17)$$

where $\mathbf{H}_s' = [\mathbf{h}_{1s}^{d\,T}\ \mathbf{h}_{2s}^{d\,T}\ \cdots\ \mathbf{h}_{(n/m)s}^{d\,T}]^T$, T is the transpose of a vector, N_I' denotes the sum of total interference power from BSs in the other cells and noise variance N_0, and $\mathbf{Q}_x$ is the $\frac{n}{m} \times \frac{n}{m}$ positive semi-definite input covariance matrix which is diagonal and satisfies $\mathrm{tr}(\mathbf{Q}_x) \le \frac{P}{m^{\alpha/2}}$. Here, the inequality holds since the rate is reduced by simply applying the same average power of each user. Due to the fact that (17) is equivalent to the right-hand side (RHS) of (11) (with a change of variables), $\Omega(l)$ is achievable in the downlink of each cell by following the same approach as that for the access routing. ■

The achievable rate of IMH protocol in dense networks will now be analyzed. The number of source nodes that can be active simultaneously is examined under the IMH protocol, while maintaining a constant throughput $\Theta(1)$ per S-D pair.

Lemma 5: When a dense network uses the IMH protocol,

$$T_n = \Omega\left(m\min\left\{l, \left(\frac{n}{m}\right)^{1/2-\epsilon}\right\}\right) \qquad (18)$$

is achievable for all $m = n^\beta$ satisfying $\beta \in [0, 1)$, where $\epsilon > 0$ is an arbitrarily small constant.

Proof: This result is obtained by modifying the analysis in [1], [14], [35] on scaling laws under our BS-based network. We mainly focus on the aspects that are different from the conventional schemes. From the 9-TDMA operation, the signal-to-interference-and-noise ratio (SINR) seen by any receiver is given by $\Omega(1)$ with a transmit power $P/n^{\alpha/2}$. It can be interpreted that when the worst case noise [30],

[31] is assumed as in the ISH protocol, the achievable throughput per S-D pair is lower-bounded by $\log(1+\text{SINR})$, thus providing a constant scaling. First consider the case $l = o(\sqrt{n/m})$ where the number l of antennas scales slower than the number n/m of nodes in a cell. Then, it is possible to activate up to l source nodes at each cell because there exist l routes for the last hop to each BS antenna in the uplink. On the other hand, when $l = \Omega(\sqrt{n/m})$, the maximum number of simultaneously transmitting sources per BS is equal to the number of routing cells on the BS boundary, which scales with $(n/m)^{1/2-\epsilon}$ for an arbitrarily small $\epsilon > 0$. Therefore, the total throughput is finally given by (18) since there are m cells in the network. ■

Throughput scalings of two conventional protocols that do not utilize the BSs are now considered. The throughputs of the MH communication [1] and the HC scheme [3] are given by

$$T_n = \Omega\left(n^{1/2-\epsilon}\right) \tag{19}$$

and

$$T_n = \Omega\left(n^{1-\epsilon}\right), \tag{20}$$

for an arbitrarily small $\epsilon > 0$, respectively. Based on the four achievability results, it is possible to obtain a lower bound on the capacity scaling in dense networks, and thus the following theorem presents the achievable rate under our BS-based routing protocols.

Theorem 1: In a dense network,

$$T_n = \Omega(n^{1-\epsilon}) \tag{21}$$

is achievable for an arbitrarily small $\epsilon > 0$.

Proof: From Lemmas 3 and 4, the achievable rate of the ISH protocol is given by

$$T_n = \Omega(ml) \tag{22}$$

for all $m = n^\beta$ satisfying $\beta \in [0, 1)$. Since (20) scales faster than (18), (19), and (22), the HC always outperforms the other protocols in dense networks. Therefore, (21) is achievable under our BS-based protocols. ■

Based on the above result, we may conclude that infrastructure does not improve the throughput scaling in dense networks.

B. Extended Networks

In the ISH protocol, the number of simultaneously transmitted sources in each cell is n/m, while only $\min\{l, \sqrt{n/m}\}$ sources can transmit simultaneously at each cell in the IMH protocol. The latter, however, has an advantage over the former in terms of better long-distance SNR or higher received signal power, i.e., more power gain, in extended (or power-limited) networks. It is demonstrated that the throughput scaling can be improved under some conditions by applying two BS-based transmissions in extended networks.

As stated in Section III, for the ISH and HC protocols, bursty transmission schemes are used in extended networks to apply the analysis for dense networks. Using the analysis similar to those used for dense networks, an achievable throughput under extended networks is given as follows.

Theorem 2: In an extended network,

$$T_n = \Omega\left(\max\left\{ml\left(\frac{m}{n}\right)^{\alpha/2-1}, m\min\left\{l, \left(\frac{n}{m}\right)^{1/2-\epsilon}\right\} n^{1/2-\epsilon}, n^{2-\alpha/2-\epsilon}\right\}\right) \tag{23}$$

is achievable for all $m = n^\beta$ satisfying $\beta \in [0, 1)$, where $\epsilon > 0$ is an arbitrarily small constant.

Proof: Under the ISH protocol, the throughput scaling decreases by $(m/n)^{\alpha/2-1}$ compared to that for dense networks, and is thus given by

$$T_n = \Omega\left(ml\left(\frac{m}{n}\right)^{\alpha/2-1}\right). \tag{24}$$

Under the IMH protocol, the same achievable throughput as that in the dense networks can be obtained, thus yielding

$$T_n = \Omega\left(m \min\left\{l, \left(\frac{n}{m}\right)^{1/2-\epsilon}\right\}\right). \tag{25}$$

From the results of [1], [3],

$$T_n = \Omega(n^{1/2-\epsilon}) \tag{26}$$

and

$$T_n = \Omega(n^{2-\alpha/2-\epsilon}) \tag{27}$$

is yielded for the MH and HC protocols, respectively. Hence, the throughput scaling in extended networks is simply lower-bounded by the maximum of (24)–(27). ■

From the achievable rates of each scheme, the interesting result below is obtained under each network condition.

Remark 1: The best achievable one among the four schemes and its scaling exponent $e(\alpha, \beta, \gamma)$ in (8) are shown in TABLE I according to the two-dimensional operating regimes on the achievable throughput scaling with respect to β and γ (see Fig. 6). This result is analyzed in Appendix A. Operating regimes A–D on the throughput scaling are shown in Fig. 6. It is important to verify the best protocol in different regimes. In Regime A, where m and l are small, the infrastructure is not helpful. In other regimes, we observe BS-based protocols are dominant in some cases depending on the path-loss exponent α. For example, Regime D has the following characteristics: the HC protocol has the highest throughput when the path-loss attenuation is small, but as the path-loss exponent α increases, the best scheme becomes the ISH protocol. This is because the penalty for long-range MIMO transmissions of the HC increases. Finally, the IMH protocol becomes dominant when α is large since the ISH protocol has a power limitation at the high path-loss attenuation regime.

V. Cut-Set Upper Bound

To see how closely the proposed schemes approach the fundamental limits in a network with infrastructure, new BS-based cut-set outer bounds on the throughput scaling are analyzed based on the information-theoretic approach [36]. Let S_L and D_L denote the sets of sources and destinations, respectively, for a given cut L in the random network. Consider the cut L dividing the network area into two halves (see Fig. 7). More precisely, under L, (wireless) source nodes S_L are on the left half of the network, while all nodes on the right half and all BS antennas are destinations D_L.[7] In this case, we get an $n \times (n + ml)$ MIMO channel between the two sets of nodes and BSs separated by the cut.

A. Dense Networks

The upper bound [3] for pure ad hoc networks of unit area is extended to our network model. Start from the following lemma.

Lemma 6: In our two-dimensional dense network where n nodes are uniformly distributed and there are m BSs with l regularly spaced antennas, the minimum distance between any two nodes or between a node and an antenna on the BS boundary is larger than $1/n^{1+\epsilon_1}$ whp for an arbitrarily small $\epsilon_1 > 0$.

Proof: This result can be obtained by slightly modifying the asymptotic analysis in [3], [14]. The minimum node-to-node distance is easily derived by following the same approach as that in [3] and is proved to scale at least as $1/n^{1+\epsilon_1}$ with probability $1 - \Theta(1/n^{2\epsilon_1})$. We now focus on how the distance between a node and an antenna on the BS boundary scales. Consider a circle of radius $1/n^{1+\epsilon_1}$ around one specific antenna on the BS boundary. Note that there are no other antennas inside the circle since the

[7]The other cut $\tilde{L}$ can also be considered in the network. In this case, sources $S_{\tilde{L}}$ represent antennas at each BS as well as ad hoc nodes on the left half. The (wireless) destination nodes $D_{\tilde{L}}$ are on the right half. Since the cut L provides a tight upper bound compared to the achievable rate, the analysis for the cut $\tilde{L}$ is not shown in this paper.

per-antenna distance is greater than $1/n^{1+\epsilon_1}$. Let $\mathcal{E}_d$ denote the event that n nodes are located outside the circle given by the antenna. Then, we have

$$P\{\mathcal{E}_d^{\mathcal{C}}\} \leq 1 - \left(1 - \frac{c_3\pi}{n^{2+2\epsilon_1}}\right)^n, \tag{28}$$

where $0 < c_3 < 1$ is a constant independent of n. Hence, by the union bound, the probability that the event $\mathcal{E}_d$ is satisfied for all the BS antennas is lower-bounded by

$$\begin{aligned} 1 - mlP\{\mathcal{E}_d^{\mathcal{C}}\} &\geq 1 - ml\left(1 - \left(1 - \frac{c_3\pi}{n^{2+2\epsilon_1}}\right)^n\right) \\ &\geq 1 - n\left(1 - \left(1 - \frac{c_3\pi}{n^{2+2\epsilon_1}}\right)^n\right), \end{aligned} \tag{29}$$

where the second inequality holds since $ml = O(n)$, which tends to one as n goes to infinity. This completes the proof. ■

Now we are ready to present the cut-set upper bound of the total throughput T_n.

Theorem 3: The total throughput T_n is upper-bounded by $n \log n$ whp in dense networks with infrastructure.

Proof: The proof essentially follows the steps similar to those of [37], [3]. Consider an S-D pair for the case where the network is divided by the cut L. The throughput per S-D pair is upper-bounded by the capacity of the SIMO channel between a source node and the rest of the network including multiple BS antennas. Hence, the total throughput for n S-D pairs is bounded by

$$\begin{aligned} T_n &\leq \sum_{i=1}^{n} \log\left(1 + \frac{P}{N_0}\left(\sum_{\substack{k=1 \\ k\neq i}}^{n} |h_{ki}|^2 + \sum_{s=1}^{m} \|\mathbf{h}_{si}^u\|^2\right)\right) \\ &\leq n \log\left(1 + \frac{P}{N_0} n^{(1+\epsilon_1)\alpha}(n - 1 + ml)\right) \\ &= \bar{c}_3 n \log n, \end{aligned} \tag{30}$$

where $\|\cdot\|$ denotes 2-norm of the vector and $\bar{c}_3 > 0$ is some constant independent of n. The second inequality holds due to Lemma 6. ■

Note that the same upper bound as that of [3] assuming no BSs is found. This upper bound means that n S-D pairs can be active with a genie-aided interference removal between simultaneously transmitting nodes, while providing power gain $\log n$. In addition, it is examined how the upper bound is close to the achievable throughput scaling.

Remark 2: In dense networks, it is easy to see that the achievable rate and the upper bound are of the same order up to a factor $\log n$. Since the achievable rate of HC scheme asymptotically approaches the upper bound within n^{ϵ}, the HC is therefore order-optimal in dense networks with the help of BSs.

B. Extended Networks

In extended networks, it is necessary to narrow down the class of S-D pairs according to their Euclidean distance to obtain a tight upper bound. In this subsection, the upper bound based on the power transfer arguments shown in [3] is shown, where an upper bound is proportional to the total received signal power from source nodes. The present problem is not equivalent to the conventional extended setup under our network model (with infrastructure support). A new upper bound based on hybrid approaches that consider either the sum of the capacities of the multiple-input single-output (MISO) channel between transmitters and each receiver or the amount of power transferred across the network according to operating regimes, is thus derived. We start from the following lemma.

Lemma 7: Assume a two-dimensional extended network where n nodes are uniformly distributed and m BSs with l antennas each are regularly spaced. When the network area with the exclusion of BS area is divided into n squares of unit area, there are less than $\log n$ nodes in each square whp.

This result can be obtained by applying our BS-based network and slightly modifying the analysis in [18]. For the cut L, the total throughput T_n for sources on the left half is bounded by the capacity of the MIMO channel between S_L and D_L, and thus

$$\begin{aligned} T_n &\le \max_{\mathbf{Q}_L \ge 0} E\left[\log\det\left(\mathbf{I}_{n+ml} + \mathbf{H}_L \mathbf{Q}_L \mathbf{H}_L^\dagger\right)\right] \\ &= \max_{\mathbf{Q}_L \ge 0} E\left[\log\det\left(\mathbf{I}_{\Theta(n)} + \mathbf{H}_L \mathbf{Q}_L \mathbf{H}_L^\dagger\right)\right], \end{aligned} \tag{31}$$

where the equality holds since $n = \Omega(ml)$.[8] $\mathbf{H}_L$ consists of $\mathbf{h}_{si}^u$ in (3) for $i \in S_L$, $s \in B$, and h_{ki} in (5) for $i \in S_L$, $k \in D_r$. Here, B and D_r represent the set of BSs in the network and (wireless) nodes on the right half, respectively. $\mathbf{Q}_L$ is the positive semi-definite input covariance matrix whose k-th diagonal element satisfies $[\mathbf{Q}_L]_{kk} \le P$ for $k \in S_L$. The set D_L of destinations is partitioned into three groups according to their location, as shown in Fig. 8. By generalized Hadamard's inequality [38] as in [16], [3],

$$\begin{aligned} T_n \ &\le \max_{\mathbf{Q}_L \ge 0} E\left[\log\det\left(\mathbf{I}_{\sqrt{n}} + \mathbf{H}_L^{(1)} \mathbf{Q}_L \mathbf{H}_L^{(1)\dagger}\right)\right] \\ &+ \max_{\mathbf{Q}_L \ge 0} E\left[\log\det\left(\mathbf{I}_{O(\sqrt{ml})} + \mathbf{H}_L^{(2)} \mathbf{Q}_L \mathbf{H}_L^{(2)\dagger}\right)\right] \\ &+ \max_{\mathbf{Q}_L \ge 0} E\left[\log\det\left(\mathbf{I}_{\Theta(n)} + \mathbf{H}_L^{(3)} \mathbf{Q}_L \mathbf{H}_L^{(3)\dagger}\right)\right], \end{aligned} \tag{32}$$

where $\mathbf{H}_L^{(t)}$ is the matrix with entries $\left[\mathbf{H}_L^{(t)}\right]_{ki}$ for $i \in S_L$, $k \in D_L^{(t)}$, and $t = 1, \cdots, 3$. Here, $D_L^{(1)}$ and $D_L^{(2)}$ denote the set of destinations located on the rectangular slab with width 1 immediately to the right of the centerline (cut) and on the ring with width 1 immediately inside each BS boundary (cut) on the left half, respectively. $D_L^{(3)}$ is given by $D_L \setminus (D_L^{(1)} \cup D_L^{(2)})$. Note that the sets ($D_L^{(1)}$ and $D_L^{(2)}$) of destinations located very close to the cut are considered separately since otherwise their contribution to the total received power will be excessive, resulting in a loose bound.

Each term in (32) will be analyzed in the theorem below. Before that, to get the total power transfer of the set $D_L^{(3)}$, the same technique as that in [3] is used, which is the relaxation of the individual power constraints to a total weighted power constraint, where the weight assigned to each source corresponds to the total received power on the other side of the cut. Specifically, each column i of the matrix $\mathbf{H}_L^{(3)}$ is normalized by the square root of the total received power on the other side of the cut from source $i \in S_L$. The total weighted power $P_{L,i}^{(3)}$ by source i is then given by

$$P_{L,i}^{(3)} = P d_{L,i}^{(3)}, \tag{33}$$

where

$$d_{L,i}^{(3)} = \sum_{k \in \bar{D}_r \setminus D_L^{(1)}} r_{ki}^{-\alpha} + \sum_{s \in B_l, t \in [1,l]} r_{si,t}^{u\ -\alpha}. \tag{34}$$

Here, $\bar{D}_r$ is the set of destination nodes including BS antennas on the right half and B_l represents the set of BSs on the left half. Then, the third term in (32) is rewritten as

$$\max_{\tilde{\mathbf{Q}}_L \ge 0} E\left[\log\det\left(\mathbf{I}_n + \mathbf{F}_L^{(3)} \tilde{\mathbf{Q}}_L \mathbf{F}_L^{(3)\dagger}\right)\right], \tag{35}$$

where $\mathbf{F}_L^{(3)}$ is the matrix with entries $\left[\mathbf{F}_L^{(3)}\right]_{ki} = \frac{1}{\sqrt{d_{L,i}^{(3)}}} \left[\mathbf{H}_L^{(3)}\right]_{ki}$, which are obtained from (34), for $i \in S_L$, $k \in D_L^{(3)}$. Then, $\tilde{\mathbf{Q}}_L$ is the matrix satisfying

$$\left[\tilde{\mathbf{Q}}_L\right]_{ki} = \sqrt{d_{L,k}^{(3)} d_{L,i}^{(3)}}\, [\mathbf{Q}_L]_{ki}, \tag{36}$$

[8] Here and in the sequel, the noise variance N_0 is assumed to be 1 to simplify the notation.

which means $\mathrm{tr}(\tilde{\mathbf{Q}}_L) \leq \sum_{i\in S_L} P_{L,i}^{(3)}$ (equal to the sum of the total received power from each source).

We next examine the behavior of the largest singular value for the normalized channel matrix $\mathbf{F}_L^{(3)}$. From the fact that $\mathbf{F}_L^{(3)}$ is well-conditioned whp, this shows how much it essentially affects an upper bound of (35), which will be analyzed in Lemma 9.

Lemma 8: Let $\mathbf{F}_L^{(3)}$ denote the normalized channel matrix whose element is given by $\left[\mathbf{F}_L^{(3)}\right]_{ki} = \frac{1}{\sqrt{d_{L,i}^{(3)}}}\left[\mathbf{H}_L^{(3)}\right]_{ki}$. Then,

$$E\left[\left\|\mathbf{F}_L^{(3)}\right\|_2^2\right] \leq \bar{c}_4(\log n)^3, \tag{37}$$

where $\|\cdot\|_2$ denotes the largest singular value of the matrix and $\bar{c}_4 > 0$ is some constant independent of n.

The proof of this lemma is presented in Appendix B. Using Lemma 8 yields the following result.

Lemma 9: The term shown in (35) is upper-bounded by

$$n^{\epsilon}\sum_{i\in S_L} P_{L,i}^{(3)} \tag{38}$$

whp where $\epsilon > 0$ is an arbitrarily small constant and $P_{L,i}^{(3)}$ is given by (33).

Proof: The proof of this lemma essentially follows that of [3]. Equation (35) is bounded by

$$\begin{aligned}&\max_{\tilde{\mathbf{Q}}_L\geq 0} E\left[\log\det\left(\mathbf{I}_n + \mathbf{F}_L^{(3)}\tilde{\mathbf{Q}}_L\mathbf{F}_L^{(3)\dagger}\right)1_{\mathcal{E}_{\mathbf{F}_L^{(3)}}}\right]\\ +&\max_{\tilde{\mathbf{Q}}_L\geq 0} E\left[\log\det\left(\mathbf{I}_n + \mathbf{F}_L^{(3)}\tilde{\mathbf{Q}}_L\mathbf{F}_L^{(3)\dagger}\right)1_{\mathcal{E}^c_{\mathbf{F}_L^{(3)}}}\right],\end{aligned} \tag{39}$$

where the event $\mathcal{E}_{\mathbf{F}_L^{(3)}}$ is given by

$$\mathcal{E}_{\mathbf{F}_L^{(3)}} = \left\{\left\|\mathbf{F}_L^{(3)}\right\|_2^2 > n^{\epsilon}\right\} \tag{40}$$

for an arbitrarily small constant $\epsilon > 0$. Then, by applying the proof technique similar to that in [3], it is possible to prove that the first term in (39) decays polynomially to zero as n tends to infinity, and for the second term in (39), it follows that

$$\begin{aligned}\max_{\tilde{\mathbf{Q}}_L\geq 0}\ & E\left[\log\det\left(\mathbf{I}_n + \mathbf{F}_L^{(3)}\tilde{\mathbf{Q}}_L\mathbf{F}_L^{(3)\dagger}\right)1_{\mathcal{E}^c_{\mathbf{F}_L^{(3)}}}\right]\\ &\leq \max_{\tilde{\mathbf{Q}}_L\geq 0} E\left[\left\|\mathbf{F}_L^{(3)}\right\|_2^2 \mathrm{tr}\left(\tilde{\mathbf{Q}}_L\right)1_{\mathcal{E}^c_{\mathbf{F}_L^{(3)}}}\right]\\ &\leq \bar{c}_4\log n \max_{\tilde{\mathbf{Q}}_L\geq 0}\mathrm{tr}\left(\tilde{\mathbf{Q}}_L\right)\\ &\leq n^{\epsilon}\sum_{i\in S_L} P_{L,i}^{(3)},\end{aligned} \tag{41}$$

where the second inequality holds by (37). ■

Note that (38) represents the power transfer from the set S_L of sources to the set $D_L^{(3)}$ of the corresponding destinations for a given cut L. For notational convenience, let $d_{L,i}^{(4)}$ and $d_{L,i}^{(5)}$ denote the first and second terms in (34), respectively. Then, $Pd_{L,i}^{(4)}$ and $Pd_{L,i}^{(5)}$ correspond to the total received power from source i to the destination sets $\bar{D}_r \setminus D_L^{(1)}$ and $D_L \setminus (D_L^{(2)} \cup \bar{D}_r)$, respectively. The computation of the total received power of the set $D_L^{(3)}$ will now be computed as follows:

$$\sum_{i\in S_L} P_{L,i}^{(3)} = \sum_{i\in S_L} Pd_{L,i}^{(4)} + \sum_{i\in S_L} Pd_{L,i}^{(5)}, \tag{42}$$

which is eventually used to compute (38).

First, to get an upper bound for $\sum_{i\in S_L} Pd_{L,i}^{(4)}$ in (42), the network area is divided into n squares of unit area. By Lemma 7, since there are less than $\log n$ nodes inside each square whp, the power transfer under the random network can be upper-bounded by that under a regular network with at most $\log n$ nodes at each square (see [3] for the detailed description). Such a modification yields the following upper bound [3] for $\sum_{i\in S_L} Pd_{L,i}^{(4)}$:

$$\sum_{i\in S_L} Pd_{L,i}^{(4)} \leq \begin{cases} \bar{c}_5 n^{2-\alpha/2}(\log n)^2 & \text{if } 2<\alpha<3 \\ \bar{c}_5\sqrt{n}(\log n)^3 & \text{if } \alpha=3 \\ \bar{c}_5\sqrt{n}(\log n)^2 & \text{if } \alpha>3 \end{cases} \tag{43}$$

whp for a constant $\bar{c}_5>0$ independent of n. Next, the second term $\sum_{i\in S_L} Pd_{L,i}^{(5)}$ in (42) can be derived as in the following lemma.

Lemma 10: The term $\sum_{i\in S_L} Pd_{L,i}^{(5)}$ is given by

$$\sum_{i\in S_L} Pd_{L,i}^{(5)} = \begin{cases} 0 & \text{if } l=o(\sqrt{n/m}) \\ O\left(nl\left(\frac{m}{n}\right)^{\alpha/2}\log n\right) & \text{if } l=\Omega(\sqrt{n/m}) \text{ and } 2<\alpha<3 \\ O\left(ml\sqrt{\frac{m}{n}}(\log n)^2\right) & \text{if } l=\Omega(\sqrt{n/m}) \text{ and } \alpha=3 \\ O\left(\frac{n}{\sqrt{l}}\left(\frac{ml}{n}\right)^{\alpha/2}\log n\right) & \text{if } l=\Omega(\sqrt{n/m}) \text{ and } \alpha>3. \end{cases} \tag{44}$$

The proof of this lemma is presented in Appendix C. It is now possible to show the proposed cut-set upper bound in extended networks.

Theorem 4: Suppose an extended network with multi-antenna BSs. Then, the total throughput T_n is upper-bounded by

$$T_n \leq \bar{c}_6 n^{\epsilon}\max\left\{nl\left(\frac{m}{n}\right)^{\alpha/2}, m\min\left\{l,\sqrt{\frac{n}{m}}\right\},\sqrt{n},n^{2-\alpha/2}\right\} \tag{45}$$

whp for all $m=n^{\beta}$ satisfying $\beta\in[0,1)$, where $\bar{c}_6$ is some constant independent of n and $\epsilon>0$ is an arbitrarily small constant.

Proof: For notational convenience, let $T_n^{(i)}$ denote the i-th term in the RHS of (32) for $i\in\{1,2,3\}$. By generalized Hadamard's inequality [38] as in [16], [3], the first term $T_n^{(1)}$ in (32) can be easily bounded by

$$\begin{aligned} T_n^{(1)} &\leq \sum_{k\in D_L^{(1)}} \log\left(1+\frac{P}{N_0}\sum_{i\in S_L}|h_{ki}|^2\right) \\ &\leq \bar{c}_7\sqrt{n}(\log n)^2, \end{aligned} \tag{46}$$

where $\bar{c}_7>0$ is a constant independent of n. Note that this upper bound does not depend on β and γ. The second inequality holds since the minimum distance between any source and destination is larger than $1/n^{1/2+\epsilon_1}$ whp for an arbitrarily small $\epsilon_1>0$, which is obtained by the derivation similar to that of Lemma 6, and there exist no more than $\sqrt{n}\log n$ nodes in $D_L^{(1)}$ whp by Lemma 7. The upper bound for $T_n^{(2)}$ is now derived. Since some nodes in $D_L^{(2)}$ are located very close to the cut and the information transfer to $D_L^{(2)}$ is limited in DoF, the second term $T_n^{(2)}$ of (32) is upper-bounded by the sum of the capacities of the MISO channels. More precisely, by generalized Hadamard's inequality,

$$\begin{aligned} T_n^{(2)} &\leq \begin{cases} \bar{c}_8 ml\log n & \text{if } l=o(\sqrt{n/m}) \\ \bar{c}_8\sqrt{nm}\log n & \text{if } l=\Omega(\sqrt{n/m}), \end{cases} \\ &\leq \bar{c}_8 m\min\left\{l,\sqrt{\frac{n}{m}}\right\}\log n \end{aligned} \tag{47}$$

where $\bar{c}_7 > 0$ is some constant independent of n. Next, the third term $T_n^{(3)}$ of (32) will be shown by using (38), (43) and Lemma 10. If $l = o(\sqrt{n/m})$, which corresponds to operating regimes A and B shown in Fig. 6, then $T_n^{(3)}$ is given by

$$T_n^{(3)} = \begin{cases} O(n^{2-\alpha/2+\epsilon}) & \text{if } 2 < \alpha < 3 \\ O(n^{1/2+\epsilon}) & \text{if } \alpha \geq 3. \end{cases} \tag{48}$$

Hence, under this network condition,

$$T_n \leq \bar{c}_6 n^{\epsilon} \max\left\{ml, \sqrt{n}, n^{2-\alpha/2}\right\}, \tag{49}$$

which is upper-bounded by the RHS of (45). Now we focus on the case for $l = \Omega(\sqrt{n/m})$ (regimes C and D in Fig. 6). In this case, $T_n^{(3)}$ is upper-bounded by

$$\begin{aligned} T_n^{(3)} &\leq \begin{cases} \bar{c}_9 n^{\epsilon}\left(n^{2-\alpha/2}(\log n)^2 + nl\left(\frac{m}{n}\right)^{\alpha/2}\log n\right) & \text{if } 2 < \alpha < 3 \\ \bar{c}_9 n^{\epsilon}\left(\sqrt{n}(\log n)^3 + ml\sqrt{\frac{m}{n}}(\log n)^2\right) & \text{if } \alpha = 3 \\ \bar{c}_9 n^{\epsilon}\left(\sqrt{n}(\log n)^2 + \frac{n}{\sqrt{l}}\left(\frac{ml}{n}\right)^{\alpha/2}\log n\right) & \text{if } \alpha > 3 \end{cases} \\ &\leq \begin{cases} \bar{c}_9 n^{\epsilon_2}\max\left\{n^{2-\alpha/2}, nl\left(\frac{m}{n}\right)^{\alpha/2}\right\} & \text{if } 2 < \alpha < 3 \\ \bar{c}_9 n^{\epsilon_2}\max\left\{\sqrt{n}, \frac{n}{\sqrt{l}}\left(\frac{ml}{n}\right)^{\alpha/2}\right\} & \text{if } \alpha \geq 3 \end{cases} \end{aligned} \tag{50}$$

for some constant $\bar{c}_9 > 0$ and an arbitrarily small constant $\epsilon_2 > \epsilon > 0$. From (46), (47), and (50), we thus get the following result:

$$\begin{aligned} T_n &\leq \begin{cases} \bar{c}_6 n^{\epsilon}\max\left\{\sqrt{nm}, n^{2-\alpha/2}, nl\left(\frac{m}{n}\right)^{\alpha/2}\right\} & \text{if } 2 < \alpha < 3 \\ \bar{c}_6 n^{\epsilon}\max\left\{\sqrt{nm}, \frac{n}{\sqrt{l}}\left(\frac{ml}{n}\right)^{\alpha/2}\right\} & \text{if } \alpha \geq 3 \end{cases} \\ &\leq \bar{c}_6 n^{\epsilon}\max\left\{\sqrt{nm}, n^{2-\alpha/2}, nl\left(\frac{m}{n}\right)^{\alpha/2}\right\}, \end{aligned} \tag{51}$$

where the first and second inequalities hold since $\sqrt{nm} = \Omega(\sqrt{n})$ and $\sqrt{nm} = \Omega\left(\frac{n}{\sqrt{l}}\left(\frac{ml}{n}\right)^{\alpha/2}\right)$, respectively, which results in (45). This completes the proof of this theorem. ■

Following the approach similar to Appendix A, it is easily shown that the scaling exponents $e(\alpha, \beta, \gamma)$ of our upper bound coincide with those shown in TABLE I according to the two-dimensional operating regimes in Fig. 6. Remark that the upper bound is the same as the result in [3], assuming no BSs, under Regime A, while it is quite different from that of [3] under other regimes. The difference comes from the fact that the information transfer by the BS antennas on the left half, i.e., the destination set $D_L^{(1)} \cup (D_L \setminus (D_L^{(2)} \cup \bar{D}_r))$, becomes dominant for large m and l. More specifically, compared to the pure network case with no BSs, as m and l increases, enough DoF gain is obtained by exploiting multiple antennas at each BS, while the power gain is provided since all the BSs are connected by the wired BS-to-BS links. Now, the relationship between achievable throughput and the cut-set upper bound is examined as follows.

Remark 3: In extended networks, it is shown that choosing the best of the four schemes ISH, IMH, MH and HC is order-optimal for all the operating regimes shown in Fig. 6 (see TABLE I). To be specific, the scaling exponent $e(\alpha, \beta, \gamma)$ for the upper bound shown in Theorem 4 is summarized as follows:

$$e(\alpha, \beta, \gamma) = \max\left\{1 + \gamma - \frac{(1-\beta)\alpha}{2}, \min\left\{\beta + \gamma, \frac{\beta+1}{2}\right\}, \frac{1}{2}, 2 - \frac{\alpha}{2}\right\}. \tag{52}$$

The first–fourth terms in (52) represent the amount of information transferred to the destination sets $D_L \setminus (D_L^{(2)} \cup \bar{D}_r)$, $D_L^{(2)}$, $D_L^{(1)}$, and $\bar{D}_r \setminus D_L^{(1)}$, and can be achieved by the ISH, IMH, MH, HC schemes, respectively. Therefore, the upper bound matches the achievable throughput scaling within n^{ϵ} in extended networks with infrastructure.

VI. Conclusion

The paper has analyzed the benefits of infrastructure support for generalized hybrid networks. Provided the number m of BSs and the number l of antennas at each BS scale at arbitrary rates relative to the number n of wireless nodes, the achievable throughput scaling and information-theoretic upper bounds were derived as a function of these scaling parameters. Specifically, two routing protocols using BSs were proposed, and their achievable scaling rates were derived and compared with that of the two conventional schemes MH and HC in both dense and extended networks. Furthermore, to assess the optimality of the achievability results, new BS-based cut-set upper bounds were derived. In both dense and extended networks, it was shown that our achievable schemes are order-optimal for all the operating regimes.

Appendix

A. Achievable Throughput in Extended Networks

Let e_{ISH}, e_{IMH}, $_{\text{MH}}$, and e_{HC} denote the scaling exponents for the achievable throughput of the ISH, IMH, MH, and HC protocols, respectively. The scaling exponents among the above schemes are compared according to operating regimes A–D shown in Fig. 6 (ϵ is omitted for notational convenience). Note that e_{ISH}, e_{MH}, and e_{HC} are given by $1+\gamma-\frac{(1-\beta)\alpha}{2}$, $\frac{1}{2}$, and $2-\frac{\alpha}{2}$, respectively, regardless of operating regimes.

1) Regime A ($0 \le \beta+\gamma < \frac{1}{2}$): $e_{\text{IMH}} = \beta+\gamma$ is obtained. Since $e_{\text{MH}} > e_{\text{IMH}} > e_{\text{ISH}}$, pure ad hoc transmissions with no BSs outperform the ISH and IMH protocols. Hence, the results in Regime A of TABLE I are obtained.
2) Regime B ($\beta+\gamma \ge \frac{1}{2}$ and $\beta+2\gamma<1$): e_{IMH} is the same as that under Regime A. Since $e_{\text{IMH}} > e_{\text{ISH}}$ and $e_{\text{IMH}} \ge e_{\text{MH}}$, the IMH always outperforms the ISH and the MH. Hence, it is found that the HC scheme has the largest scaling exponent under $2<\alpha<4-2\beta-2\gamma$, but if $\alpha \ge 4-2\beta-2\gamma$ the IMH protocol becomes the best.
3) Regime C ($\beta+2\gamma \ge 1$ and $\gamma < \frac{1}{2}(\beta^2-3\beta+2)$): Remark that $e_{\text{IMH}} = \frac{1+\beta}{2}$ and $e_{\text{IMH}} \ge e_{\text{MH}}$. Then, the following inequalities with respect to the path-loss exponent α are found: $e_{\text{ISH}} > e_{\text{IMH}}$ for $2<\alpha<1+\frac{2\gamma}{1-\beta}$ and $e_{\text{ISH}} \le e_{\text{IMH}}$ for $\alpha \ge 1+\frac{2\gamma}{1-\beta}$; $e_{\text{HC}} > e_{\text{IMH}}$ for $2<\alpha<3-\beta$ and $e_{\text{HC}} \le e_{\text{IMH}}$ for $\alpha \ge 3-\beta$; and $e_{\text{HC}} > e_{\text{ISH}}$ for $2<\alpha<\frac{2(1-\gamma)}{\beta}$ and $e_{\text{HC}} \le e_{\text{ISH}}$ for $\alpha \ge \frac{2(1-\gamma)}{\beta}$. The best scheme thus depends on the comparison among $1+\frac{2\gamma}{1-\beta}$, $3-\beta$, and $\frac{2(1-\gamma)}{\beta}$. Note that $3-\beta < \frac{2(1-\gamma)}{\beta}$ and $3-\beta > 1+\frac{2\gamma}{1-\beta}$ always hold under Regime C. Finally, the best achievable schemes with respect to α are obtained and are shown in Fig. 9(a).
4) Regime D ($\beta+\gamma<1$ and $\gamma \ge \frac{1}{2}(\beta^2-3\beta+2)$): The same scaling exponents for our four protocols are the same as those under Regime C. The result is obtained by comparing $1+\frac{2\gamma}{1-\beta}$, $3-\beta$, and $\frac{2(1-\gamma)}{\beta}$ under Regime D. The following two inequalities $3-\beta \ge \frac{2(1-\gamma)}{\beta}$ and $3-\beta \le 1+\frac{2\gamma}{1-\beta}$ are satisfied, and the best achievable schemes with respect to α are obtained and shown in Fig. 9(b).

This coincides with the result shown in TABLE I.

B. Proof of Lemma 8

The size of matrix $\mathbf{F}_L^{(3)}$ is $\Theta(n)\times\Theta(n)$ since $ml = O(n)$. Thus, the analysis essentially follows the argument in [3] with a slight modification (see Appendix III in [3] for more precise description). Consider the network transformation resulting in a regular network with at most $\log n$ nodes at each square vertex except for the area covered by BSs. Then, the same node displacement as shown in [3] is performed, which will decrease the Euclidean distance between source and destination nodes. For convenience, the source node positions are indexed in the resulting regular network. It is thus assumed that the source nodes under the cut are located at positions $(-i_x+1, i_y)$ where $i_x, i_y = 1, \cdots \sqrt{n}$. In the following,

$\sum_{k\in D_L^{(3)}} \left|\left[\mathbf{F}_L^{(3)}\right]_{ki}\right|^2$ and an upper bound for $\sum_{i\in S_L} \left|\left[\mathbf{F}_L^{(3)}\right]_{ki}\right|^2$ are derived:

$$\begin{aligned}\sum_{k\in D_L^{(3)}} \left|\left[\mathbf{F}_L^{(3)}\right]_{ki}\right|^2 &= \sum_{k\in D_L^{(3)}} \left|\frac{1}{\sqrt{d_{L,i}^{(3)}}}\left[\mathbf{H}_L^{(3)}\right]_{ki}\right|^2 \\ &= \frac{\sum_{k\in D_L^{(3)}} \left|\left[\mathbf{H}_L^{(3)}\right]_{ki}\right|^2}{\sum\limits_{k\in \bar{D}_r\setminus D_L^{(1)}} r_{ki}^{-\alpha} + \sum\limits_{s\in B_l, t\in[1,l]} r_{si,t}^{u\ -\alpha}} \\ &= 1, \end{aligned} \tag{53}$$

where $\bar{D}_r$ is the set of nodes including BS antennas on the right half and the second equality comes from (34), and

$$\begin{aligned}\sum_{i\in S_L} \left|\left[\mathbf{F}_L^{(3)}\right]_{ki}\right|^2 &= \sum_{i\in S_L} \left|\frac{1}{\sqrt{d_{L,i}^{(3)}}}\left[\mathbf{H}_L^{(3)}\right]_{ki}\right|^2 \\ &= \begin{cases} \sum\limits_{i\in S_L} \frac{r_{ki}^{-\alpha}}{d_{L,i}^{(3)}} & \text{if } k\in \bar{D}_r\setminus D_L^{(1)} \\ \sum\limits_{i\in S_L} \frac{r_{si,t}^{u\ -\alpha}}{d_{L,i}^{(3)}} & \text{if } k\in \{t: t\in[1,l] \text{ for } s\in B_l\} \end{cases} \\ &\le \begin{cases} \sum\limits_{i\in S_L} \frac{r_{ki}^{-\alpha}}{\sum\limits_{k\in\bar{D}_r\setminus D_L^{(1)}} r_{ki}^{-\alpha}} & \text{if } k\in \bar{D}_r\setminus D_L^{(1)} \\ \sum\limits_{i\in S_L} \frac{r_{si,t}^{u\ -\alpha}}{\sum\limits_{k\in\bar{D}_r\setminus D_L^{(1)}} r_{ki}^{-\alpha}} & \text{if } k\in \{t: t\in[1,l] \text{ for } s\in B_l\} \end{cases} \\ &\le \begin{cases} \bar{c}_{10}\log n \sum\limits_{i\in S_L} x_i^{\alpha-2} r_{ki}^{-\alpha} & \text{if } k\in \bar{D}_r\setminus D_L^{(1)} \\ \bar{c}_{10}\log n \sum\limits_{i\in S_L} x_i^{\alpha-2} r_{si,t}^{u\ -\alpha} & \text{if } k\in \{t: t\in[1,l] \text{ for } s\in B_l\} \end{cases} \\ &\le \begin{cases} \bar{c}_{10}\log n \sum\limits_{i\in S_L} r_{ki}^{-2} & \text{if } k\in \bar{D}_r\setminus D_L^{(1)} \\ \bar{c}_{10}\log n \sum\limits_{i\in S_L} r_{si,t}^{u\ -2} & \text{if } k\in \{t: t\in[1,l] \text{ for } s\in B_l\} \end{cases} \\ &\le \bar{c}_{10}(\log n)^2 \sum_{i_x,i_y=1}^{\sqrt{n}} \frac{1}{i_x^2+i_y^2} \\ &\le \bar{c}_{11}(\log n)^3, \end{aligned} \tag{54}$$

where B_l is the set of BSs in the left half network, $\bar{c}_{10} > 0$ and $\bar{c}_{11} > 0$ are some constants, and x_i denotes the x-coordinate of node $i \in S_L$ for our random network ($x_i = 1, \cdots, \sqrt{n}$). Here, the second and fifth inequalities hold since

$$\sum_{k\in\bar{D}_r\setminus D_L^{(1)}} r_{ki}^{-\alpha} \ge \frac{x_i^{2-\alpha}}{\bar{c}_{10}\log n} \tag{55}$$

and

$$\sum_{i_x,i_y=1}^{\sqrt{n}} \frac{1}{i_x^2+i_y^2} = O(\log n), \tag{56}$$

respectively (see [3] for the detailed derivation). The third inequality comes from the result of Lemma 7. Hence, it is proved that both scaling results are the same as the random network case shown in [3]. Now it is possible to prove the inequality in (37). Following the same line as that in [3], we thus have

$$E\left[\mathrm{tr}\left(\left(\mathbf{F}_L^{(3)\dagger}\mathbf{F}_L^{(3)}\right)^q\right)\right] \le C_q n\left(\bar{c}_{12}\log n\right)^{3q}, \tag{57}$$

where $C_q = \frac{(2q)!}{q!(q+1)!}$ is the Catalan number for any q and $\bar{c}_{12} > 0$ is a constant independent of n. Then, from the property $\|\mathbf{F}_L^{(3)}\|_2^2 = \lim_{q\to\infty}\mathrm{tr}((\mathbf{F}_L^{(3)\dagger}\mathbf{F}_L^{(3)})^q)^{1/q}$ (see [39]), the expectation of the term $\|\mathbf{F}_L^{(3)}\|_2^2$ is upper-bounded by

$$\begin{aligned} E\left[\left\|\mathbf{F}_L^{(3)}\right\|_2^2\right] &\le \lim_{q\to\infty}\left(E\left[\mathrm{tr}\left(\left(\mathbf{F}_L^{(3)\dagger}\mathbf{F}_L^{(3)}\right)^q\right)\right]\right)^{1/q} \\ &\le \lim_{q\to\infty}\left(C_q n\left(\bar{c}_{12}\log n\right)^{3q}\right)^{1/q} \\ &= 4(\bar{c}_{12}\log n)^3, \end{aligned} \tag{58}$$

where the equality holds since $\lim_{q\to\infty} C_q^{1/q} = 4$. Here, the first inequality comes from dominated convergence theorem and Jensen's inequality. This completes the proof.

C. Proof of Lemma 10

When $l = o(\sqrt{n/m})$, there is no destination in $D_L^{(5)}$, and thus $\sum_{i\in S_L} Pd_{L,i}^{(5)}$ becomes zero. Hence, the case for $l = \Omega(\sqrt{n/m})$ is the focus from now on. By the same argument as shown in the derivation of $\sum_{i\in S_L} Pd_{L,i}^{(4)}$, the network area is divided into n squares of unit area. Then, by Lemma 7, the power transfer under our random network can be upper-bounded by that under a regular network with at most $\log n$ nodes at each square except for the area covered by BSs. As illustrated in Fig. 10, the nodes in each square are moved together onto one vertex of the corresponding square. The node displacement is performed in a sense of decreasing the Euclidean distance between node $i \in S_L$ and the antennas of the corresponding BS, thereby providing an upper bound for $d_{L,i}^{(5)}$. Layers of each cell are then introduced, as shown in Fig. 10, where there exist $8(\epsilon_0\sqrt{n/m}+k)$ vertices, each of which includes $\log n$ nodes, in the k-th layer l'_k of each cell. The regular network described above can also be transformed into the other, which contains antennas regularly placed at spacing $\epsilon_0\sqrt{\frac{n\pi}{ml}}$ outside the shaded square for arbitrarily small $\epsilon_0 > 0$. Note that the shaded square of size $2k \times 2k$ is drawn based on a source node in l'_k at its center (see Fig. 10). The modification yields an increase of the term $d_{L,i}^{(5)}$ by source i. When $d_{L,i(k)}^{(5)}$ is defined as $d_{L,i}^{(5)}$ by node i that lies in l'_k, the following upper bound for $d_{L,i(k)}^{(5)}$ is obtained:

$$\begin{aligned} d_{L,i(k)}^{(5)} &\le \sum_{k_x,k_y=\zeta}^{\infty} \frac{1}{\left(\left(\epsilon_0\sqrt{\frac{n\pi}{ml}}k_x\right)^2 + \left(\epsilon_0\sqrt{\frac{n\pi}{ml}}k_y\right)^2\right)^{\alpha/2}} \\ &= \left(\frac{ml}{n}\right)^{\alpha/2}\sum_{k_x,k_y=\zeta}^{\infty}\frac{c_4^\alpha}{(k_x^2+k_y^2)^{\alpha/2}} \\ &= \left(\frac{ml}{n}\right)^{\alpha/2}\sum_{k'=\zeta}^{\infty}\frac{8c_4^\alpha k'}{k'^\alpha} \\ &\le \bar{c}_{13}\left(\frac{ml}{n}\right)^{\alpha/2}\left(\frac{1}{\zeta^{\alpha-1}} + \int_\zeta^\infty \frac{1}{x^{\alpha-1}}dx\right) \\ &\le \bar{c}_{13}\left(1+\frac{1}{\alpha-2}\right)\left(\frac{ml}{n}\right)^{\alpha/2}\frac{1}{\zeta^{\alpha-2}}, \end{aligned} \tag{59}$$

where $\zeta = 1 + \lfloor kc_4 \rfloor$, $c_4 = \frac{1}{\epsilon_0}\sqrt{\frac{ml}{n\pi}}$, and $\bar{c}_{13}$ is some constant independent of n. Here, $\lfloor x \rfloor$ denotes the greatest integer less than or equal to x. Hence, $d^{(5)}_{L,i(k)}$ is given by

$$d^{(5)}_{L,i(k)} = \begin{cases} O\left(\left(\frac{ml}{n}\right)^{\alpha/2}\right) & \text{if } k = O\left(\sqrt{\frac{n}{ml}}\right) \\ O\left(k^{2-\alpha}\left(\frac{ml}{n}\right)\right) & \text{if } k = \Omega\left(\sqrt{\frac{n}{ml}}\right), \end{cases} \tag{60}$$

finally yielding

$$\begin{aligned} \sum_{i \in S_L} P d^{(5)}_{L,i} &\leq P\frac{m}{2}\log n \sum_{k=1}^{\sqrt{n/m}} 8\left(\epsilon_0\sqrt{\frac{n}{m}} + k\right) d^{(5)}_{L,i(k)} \\ &\leq \bar{c}_{14} P\sqrt{nm}\log n \left[\sum_{k=1}^{\sqrt{n/ml}-1}\left(\frac{ml}{n}\right)^{\alpha/2} + \sum_{k=\sqrt{n/ml}}^{\sqrt{n/m}} k^{2-\alpha}\left(\frac{ml}{n}\right)\right] \\ &\leq \bar{c}_{14} P\sqrt{nm}\log n \left[\left(\frac{ml}{n}\right)^{(\alpha-1)/2} + \left(\frac{ml}{n}\right)\left(\left(\frac{ml}{n}\right)^{\alpha/2-1} + \int_{\sqrt{n/ml}}^{\sqrt{n/m}} \frac{1}{k^{\alpha-2}} dx\right)\right] \\ &\leq \begin{cases} \frac{3\bar{c}_{14}P}{3-\alpha} nl\left(\frac{m}{n}\right)^{\alpha/2}\log n & \text{if } 2 < \alpha < 3 \\ \frac{3\bar{c}_{14}P}{2} ml\sqrt{\frac{m}{n}}(\log n)^2 & \text{if } \alpha = 3 \\ \frac{3\bar{c}_{14}P}{\alpha-3}\frac{n}{\sqrt{l}}\left(\frac{ml}{n}\right)^{\alpha/2}\log n & \text{if } \alpha > 3, \end{cases} \end{aligned} \tag{61}$$

where $\bar{c}_{14}$ is some constant independent of n. Here, the first inequality holds since there exist $8(\epsilon_0\sqrt{n/m} + k)$ vertices in l'_k and at most $\log n$ nodes at each vertex. Equation (61) yields the result in (44).

REFERENCES

[1] P. Gupta and P. R. Kumar, "The capacity of wireless networks," *IEEE Trans. Inf. Theory*, vol. 46, pp. 388–404, Mar. 2000.

[2] D. E. Knuth, "Big Omicron and big Omega and big Theta," *ACM SIGACT News*, vol. 8, pp. 18–24, Apr.-June 1976.

[3] A. Özgür, O. Lévêque, and D. N. C. Tse, "Hierarchical cooperation achieves optimal capacity scaling in ad hoc networks," *IEEE Trans. Inf. Theory*, vol. 53, pp. 3549–3572, Oct. 2007.

[4] U. Niesen, P. Gupta, and D. Shah, "On capacity scaling in arbitrary wireless networks," *IEEE Trans. Inf. Theory*, submitted for publication.

[5] L.-L. Xie, "On information-theoretic scaling laws for wireless networks," *IEEE Trans. Inf. Theory*, submitted for publication.

[6] U. Niesen, P. Gupta, and D. Shah, "The capacity region of large wireless networks," *IEEE Trans. Inf. Theory*, submitted for publication.

[7] M. Grossglauser and D. N. C. Tse, "Mobility increases the capacity of ad hoc wireless networks," *IEEE/ACM Trans. Networking*, vol. 10, pp. 477–486, Aug. 2002.

[8] V. R. Cadambe and S. A. Jafar, "Interference alignment and degrees of freedom of the K user interference channel," *IEEE Trans. Inf. Theory*, vol. 54, pp. 3425–3441, Aug. 2008.

[9] A. Zemlianov and G. de Veciana, "Capacity of ad hoc wireless networks with infrastructure support," *IEEE J. Select. Areas Commun.*, vol. 23, pp. 657–667, Mar. 2005.

[10] S. R. Kulkarni and P. Viswanath, "Throughput scaling for heterogeneous networks," in *Proc. IEEE Int. Symp. Inf. Theory (ISIT)*, Yokohama, Japan, June/July 2003, p. 452.

[11] U. C. Kozat and L. Tassiulas, "Throughput capacity of random ad hoc networks with infrastructure support," in *Proc. ACM MobiCom*, San Diego, CA, Sept. 2003, pp. 55–65.

[12] B. Liu, Z. Liu, and D. Towsley, "Capacity of a wireless ad hoc network with infrastructure," preprint.

[13] B. Liu, P. Thiran, and D. Towsley, "Capacity of a wireless ad hoc network with infrastructure," in *Proc. ACM MobiHoc*, Montréal, Canada, Sept. 2007.

[14] A. El Gamal, J. Mammen, B. Prabhakar, and D. Shah, "Optimal throughput-delay scaling in wireless networks-Part I: The fluid model," *IEEE Trans. Inf. Theory*, vol. 52, pp. 2568–2592, June 2006.

[15] L.-L. Xie and P. R. Kumar, "A network information theory for wireless communication: scaling laws and optimal operation," *IEEE Trans. Inf. Theory*, vol. 50, pp. 748–767, May 2004.

[16] A. Jovicic, P. Viswanath, and S. R. Kulkarni, "Upper bounds to transport capacity of wireless networks," *IEEE Trans. Inf. Theory*, vol. 50, pp. 2555–2565, Nov. 2004.

[17] F. Xue, L.-L. Xie, and P. R. Kumar, "The transport capacity of wireless networks over fading channels," *IEEE Trans. Inf. Theory*, vol. 51, pp. 834–847, Mar. 2005.

[18] M. Franceschetti, O. Dousse, D. N. C. Tse, and P. Thiran, "Closing the gap in the capacity of wireless networks via percolation theory," *IEEE Trans. Inf. Theory*, vol. 53, pp. 1009–1018, Mar. 2007.

[19] A. Özgür, R. Johari, D. N. C. Tse, and O. Lévêque, "Information theoretic operating regimes of large wireless networks," *IEEE Trans. Inf. Theory*, submitted for publication.

[20] O. Lévêque and İ. E. Telatar, "Information-theoretic upper bounds on the capacity of large extended ad hoc wireless networks," *IEEE Trans. Inf. Theory*, vol. 51, pp. 858–865, Mar. 2005.

[21] A. Özgür, O. Lévêque, and E. Preissmann, "Scaling laws for one- and two-dimensional random wireless networks in the low-attenuation regime," *IEEE Trans. Inf. Theory*, vol. 53, pp. 3573–3585, Oct. 2007.

[22] M. K. Varanasi and T. Guess, "Optimum decision feedback multiuser equalization with successive decoding achieves the total capacity of the Gaussian multiple-access channel," in *Proc. Asilomar Conf. on Signals, Systems and Computers*, Pacific Grove, CA, Nov. 1997, pp. 1405–1409.

[23] P. Viswanath and D. N. C. Tse, "Sum capacity of the vector Gaussian broadcast channel and uplink-downlk duality," *IEEE Trans. Inf. Theory*, vol. 49, pp. 1912–1921, Aug. 2003.

[24] D. Tse and P. Viswanath, *Fundamentals of Wireless Communication*. New York: Cambridge University Press, 2005.

[25] M. H. M. Costa, "Writing on dirty paper," *IEEE Trans. Inf. Theory*, vol. IT-29, pp. 439–441, May 1983.

[26] G. Caire and S. Shamai (Shitz), "On the achievable throughput in multiantenna broadcast channel," *IEEE Trans. Inf. Theory*, vol. 49, pp. 1691–1706, July 2003.

[27] H. Weingarten, Y. Steinberg, and S. Shamai (Shitz), "The capacity region of the Gaussian multiple-input multiple-output broadcast channel," *IEEE Trans. Inf. Theory*, vol. 52, pp. 3936–3964, Sept. 2006.

[28] H. El Gamal, "On the scaling laws of dense wireless sensor networks: the data gathering channel," *IEEE Trans. Inf. Theory*, vol. 51, pp. 1229–1234, Mar. 2005.

[29] A. Giridhar and P. R. Kumar, "Computing and communicating functions over sensor networks," *IEEE J. Select. Areas Commun.*, vol. 23, pp. 755–764, Apr. 2005.

[30] M. Médard, "The effect upon channel capacity in wireless communications of perfect and imperfect knowledge of the channel," *IEEE Trans. Inf. Theory*, vol. 46, pp. 933–946, May 2000.

[31] B. Hassibi and B. M. Hochwald, "How much training is needed in multiple-antenna wireless links?" *IEEE Trans. Inf. Theory*, vol. 49, pp. 951–963, Apr. 2003.

[32] J. Kahane, *Some Random Series of Functions*. Cambridge: Cambridge University Press, 1985.

[33] S. Viswanath, N. Jindal, and A. Goldsmith, "Duality, achievable rates, and sum-rate capacity of Gaussian MIMO broadcast channels," *IEEE Trans. Inf. Theory*, vol. 49, pp. 2658–2668, Oct. 2003.

[34] W. Yu, "Uplink-downlink duality via minimax duality," *IEEE Trans. Inf. Theory*, vol. 52, pp. 361–374, Feb. 2006.

[35] W.-Y. Shin, S.-Y. Chung, and Y. H. Lee, "Improved power-delay trade-off in wireless ad hoc networks using opportunistic routing," in *Proc. IEEE Int. Symp. Inf. Theory (ISIT)*, Nice, France, June 2007, pp. 841–845.

[36] T. M. Cover and J. A. Thomas, *Elements of Information Theory*. New York: Wiley, 1991.

[37] M. Gastpar and M. Vetterli, "On the capacity of large Gaussian relay networks," *IEEE Trans. Inf. Theory*, vol. 51, pp. 765–779, Mar. 2005.

[38] F. Constantinescu and G. Scharf, "Generalized Gram-Hadamard inequality," *Journal of Inequalities and Applications*, vol. 2, pp. 381–386, 1998.

[39] R. A. Horn and C. R. Johnson, *Matrix Analysis*. Cambridge, U. K.: Cambridge University Press, 1999.

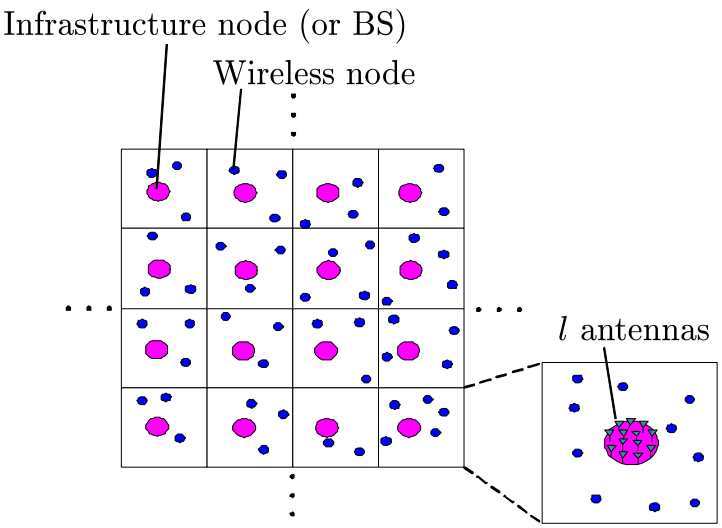

Fig. 1. The wireless ad hoc network with infrastructure support.

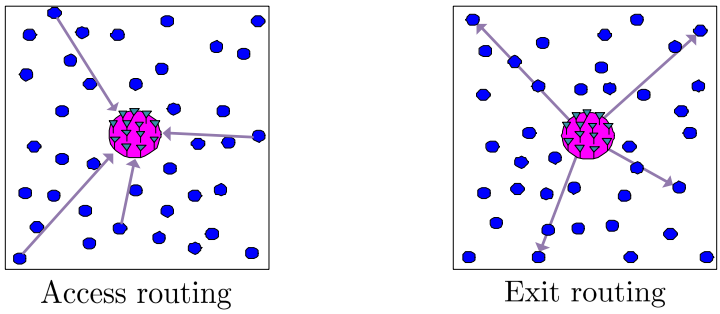

Fig. 2. The infrastructure-supported single-hop (ISH) protocol.

TABLE I

ACHIEVABLE RATES FOR AN EXTENDED NETWORK WITH INFRASTRUCTURE.

Regime	Condition	Scheme	$e(\alpha,\beta,\gamma)$
A	$2<\alpha<3$	HC	$2-\frac{\alpha}{2}$
	$\alpha\geq 3$	MH	$\frac{1}{2}$
B	$2<\alpha<4-2\beta-2\gamma$	HC	$2-\frac{\alpha}{2}$
	$\alpha\geq 4-2\beta-2\gamma$	IMH	$\beta+\gamma$
C	$2<\alpha<3-\beta$	HC	$2-\frac{\alpha}{2}$
	$\alpha\geq 3-\beta$	IMH	$\frac{1+\beta}{2}$
D	$2<\alpha<\frac{2(1-\gamma)}{\beta}$	HC	$2-\frac{\alpha}{2}$
	$\frac{2(1-\gamma)}{\beta}\leq\alpha<1+\frac{2\gamma}{1-\beta}$	ISH	$1+\gamma-\frac{\alpha(1-\beta)}{2}$
	$\alpha\geq 1+\frac{2\gamma}{1-\beta}$	IMH	$\frac{1+\beta}{2}$

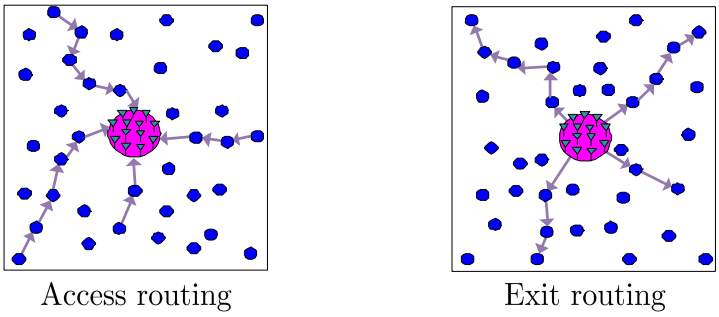

Fig. 3. The infrastructure-supported multi-hop (IMH) protocol.

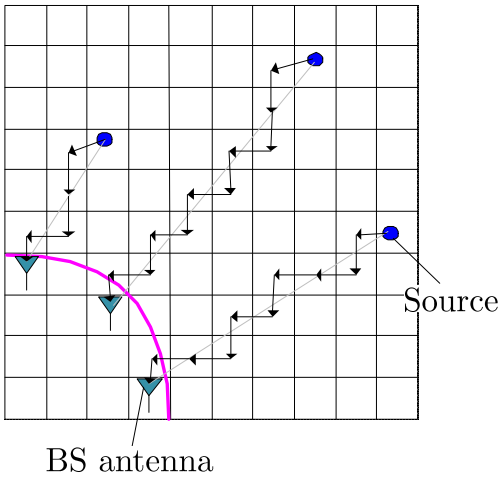

Fig. 4. The access routing in the IMH protocol.

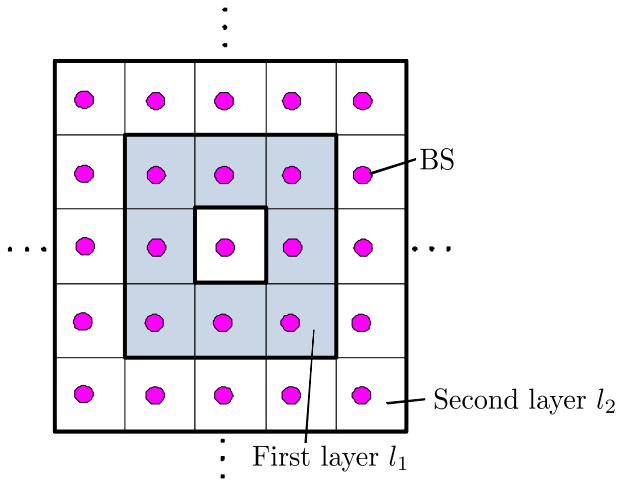

Fig. 5. Grouping of interfering cells. The first layer l_1 of the network represents the outer 8 shaded cells.

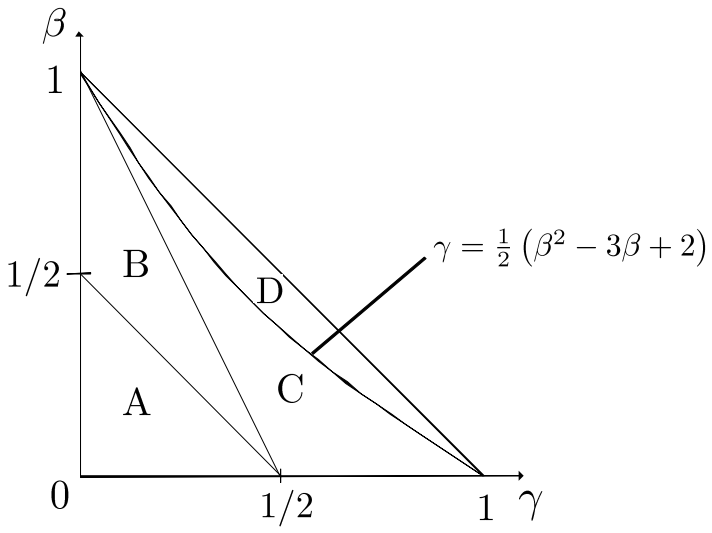

Fig. 6. Operating regimes on the achievable throughput scaling with respect to β and γ.

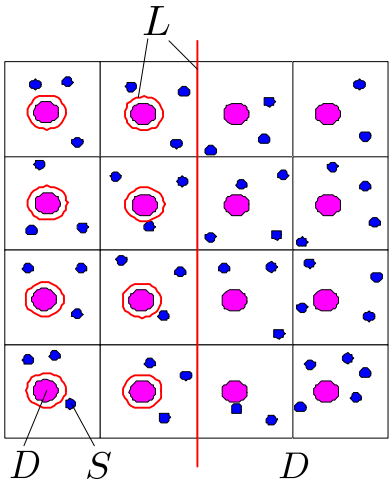

Fig. 7. The cut-set L in the two-dimensional random network.

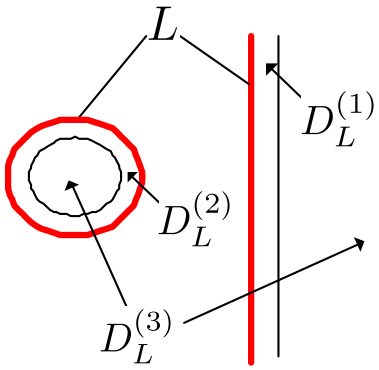

Fig. 8. The partition of destinations in the two-dimensional random network. To simplify the figure, one BS is shown in the left half network.

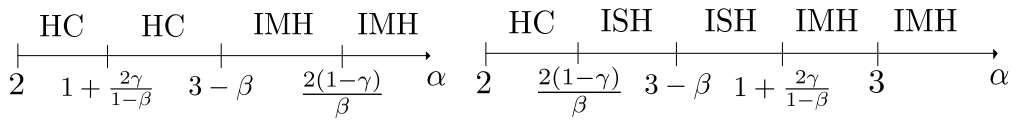

(a) (b)

Fig. 9. The best achievable schemes with respect to α. (a) The Regime C. (b) The Regime D.

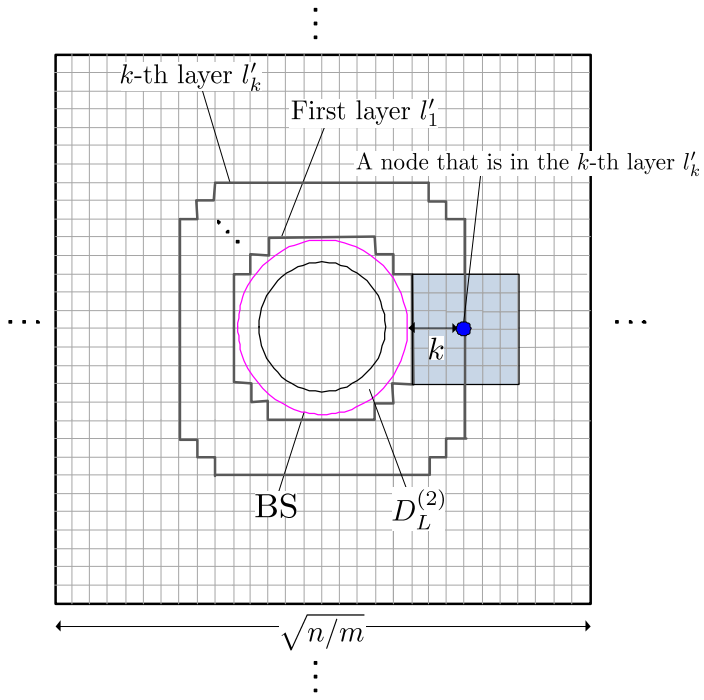

Fig. 10. The displacement of the nodes to square vertices. The antennas are regularly placed at spacing $\sqrt{\frac{n}{ml}}$ outside the shaded square.